

Emulsion Polymerization of Novel Transparent Latices by Pulsed Electron Beam Initiation

Jens Pusch and Alex M. van Herk*

Laboratory of Polymer Chemistry, Eindhoven University of Technology, P.O. Box 513, 5600 MB Eindhoven, The Netherlands

Received January 31, 2005; Revised Manuscript Received June 8, 2005

ABSTRACT: The use of electron irradiation as an alternative to chemical initiation in emulsion polymerization is a well-known but not widely used technique. The pulsed electron beam polymerization (PEBP) allows the synthesis of unique latices with small particle sizes at low surfactant concentrations. PEBP of methyl methacrylate (MMA), ethyl methacrylate (EMA), butyl methacrylate (BMA), vinyl acetate (VAc), and styrene (Sty) was performed with regard to the production of transparent latices at low surfactant concentrations. The development of novel polymers with the focus on bio- and nanomaterials is intensely investigated nowadays, and the developed latices might find an application in this area. The reason for the formation of small sized latex particles was identified in the high radical flux applied to the system by the high-frequency pulsed electron beam (PEB) resulting in a high degree of low molecular weight polymeric material. The presence of hydroxy-functionalized polymer chains seems to colloiddally stabilize small latex particles and prevent coagulation even at low surfactant concentrations. A high k_p in combination with a good water solubility of the monomer enhanced the possibility for the formation of transparent latices by PEBP.

Introduction

Emulsion polymerization is nowadays a very important industrial process, and around 4% (based on dry polymer) of the total amount of synthetic polymers is produced by emulsion polymerization.¹ The search for novel latices with unique product properties is very challenging. The commercially produced generally opaque latices are used in the paint and adhesive area. Transparent latices might find an application in the field of the growing market for optical and biomedical materials. The synthesis of transparent latices with small particle sizes can nowadays be achieved by emulsion polymerization or microemulsion polymerization. High amounts of surfactant are needed to obtain and stabilize the small particle sizes.² In some application fields like the biomedical sector the presence of high amounts of small molecules that can migrate into the surrounding tissue is not desirable. The surfactants have to be removed by rather time-consuming procedures, which can result in a considerable decrease of the latex stability and transparency. A possibility to overcome these problems is the pulsed electron beam polymerization (PEBP) toward transparent latices. Radicals produced through chemical initiation today predominantly initiate emulsion polymerizations. High-energy radiation (HER) like γ , ultrasound, and pulsed electron beam (PEB) irradiation have been intensively investigated; they are not commonly used as initiation methods.³ An interesting feature of the PEBP is the controllable and stable flux of radicals, which depends on the irradiation intensity. In PEBP a constant, a large quantity of radicals is created with every pulse, and the radical concentration is much higher than in the steady state of a chemically initiated system. Hence, a large number of particles with polymer chains of fairly low molecular weight will be formed. Another stabilization factor in the PEBP at low surfactant concentrations is

the high degree of OH-functionalized polymer chains.⁴ A major initiating species in the PEBP are OH radicals formed by the radiolysis of water. The OH radicals initiate polymerization and form oligomer chains with hydroxyl functions. In microemulsion polymerizations short-chained hydroxyl-functionalized molecules, like e.g. 1-pentanol, are added to the recipe as a cosurfactant to obtain small particle sizes.² Because this in-situ formed cosurfactant is also the precursor material for the growing polymeric chains, the hydrophilic hydroxyl-functionalized end groups, predominantly present on the latex surface, will finally also increase the colloidal stability of the latex. Another interesting factor is that the ionic strength of the water phase in the PEBP is very low because no salts (in the form of initiators) are required. In theory, the absence of electrolyte improves the colloidal stability of more and smaller particles.

The aim of the work described was to investigate whether PEBP could be a feasible tool for the production of transparent latices with small particle sizes. Previous investigations showed the influence of the hydrophilicity of the investigated monomer onto the initiation mechanism in PEBP.⁴ Therefore, in this study the hydrophilicity was varied by choosing the monomers MMA, EMA, BMA, VAc, and Sty. The factors that affect the stabilization of transparent latices formed in PEBP are another topic investigated within this research.

Experimental Section

Characterization. Dynamic light scattering (DLS) was performed on a Malvern 4700 light scattering apparatus with a 488 nm laser, a Malvern 7032 correlator, a PCS7 stepper motor controller, and a PCS8 temperature controller. The scattering angle was 90° and the measuring temperature 25 °C. The intensity weighed mean-average diameter was measured 30 times to arrive at an average value. TEM measurements indicated that the actual particle size is lower than measured with DLS. Molecular weight distributions (MWDs) were measured by SEC at room temperature using a Waters SEC equipped with a Waters model 510 pump and a model

* Corresponding author: e-mail a.m.v.herk@tue.nl.

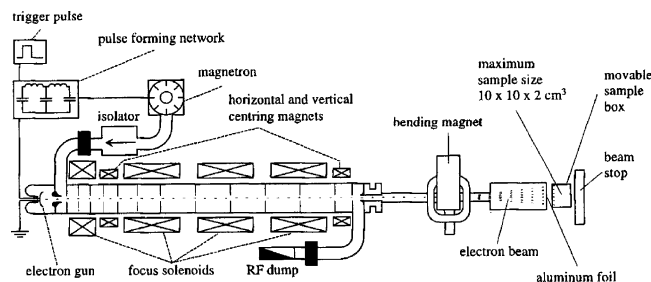


Figure 1. Schematic drawing of the linear electron accelerator as used in the setup.¹¹

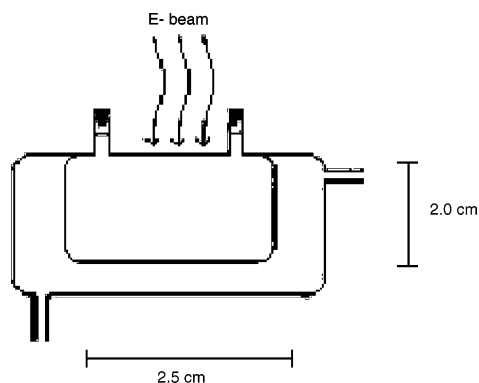


Figure 2. Schematic drawing of the PEBP reactor.

410 differential refractometer (40 °C). THF was used as the eluent at a flow rate of 1.0 mL/min. A set of two linear columns (Mixed-C, Polymer Laboratories, 30 cm, 40 °C) was used. Calibration was carried out using narrow MWD of PSty standards ranging from 600 to 7×10^6 g/mol. The molecular weights were calculated using the universal calibration principle and Mark-Houwink parameters (PMMA: $K = 9.55 \times 10^{-5}$ dL/g, $a = 0.719$; PSty: $K = 1.14 \times 10^{-4}$ dL/g, $a = 0.716$; PEMA: $K = 9.7 \times 10^{-5}$ dL/g, $a = 0.714$; PBMA: $K = 1.48 \times 10^{-4}$ dL/g, $a = 0.664$; PVAc: $K = 2.24 \times 10^{-4}$ dL/g, $a = 0.674$).⁵ Data acquisition and processing were performed using Waters Millennium 32 software.

Materials. The monomers methyl methacrylate (MMA, 99%, Aldrich) ethyl methacrylate (EMA, 99%, Aldrich), butyl methacrylate (BMA, 99%, Aldrich), vinyl acetate (VAc 99%, Aldrich), and styrene (Sty, 99%, Merck) were used after being purified from inhibitor by passing them over a column filled with an inhibitor remover package (Aldrich). Sodium dodecyl sulfate (SDS, 96.0%, Fluka) and sodium peroxodisulfate (SPS, 99+%, Merck) were used as received. Deionized water was used in all experiments.

Setup. The Eindhoven Technical University's linear accelerator was used to initiate the polymerization reaction. The accelerated electrons had an energy of 5 MeV. The accelerator is a substantially modified Philips SL 75-5 medical accelerator. Accelerated electrons left the vacuum through a 100 μ m aluminum foil scattering the electrons over a mean angle of 8°. The target was placed at a distance of 5 cm from the aluminum foil. The pulse width was 4 μ s. The pulse repetition rate was varied between 10, 25, and 50 Hz. Further details can be found in the literature.⁶⁻⁸

A schematic drawing is shown in Figure 1.

For the batch reactions a cylindrical, thermostated, double wall quartz cell of 5 mL volume was used. The inner cell had a diameter of 2.5 cm and a height of 2 cm. A thermostat controlled the temperature of the reactor. After addition of the emulsion the cell was sealed with plastic sealing caps. The cell was fixed in a Lab-Line multiwrist shaker. A schematic drawing of the cell is shown in Figure 2.

PEB Polymerization. In a typical batch polymerization procedure, 4.5 mL of deionized water, 0.5 g of monomer, and 0.015 g of surfactant were emulsified for 5 min on a Whirli-

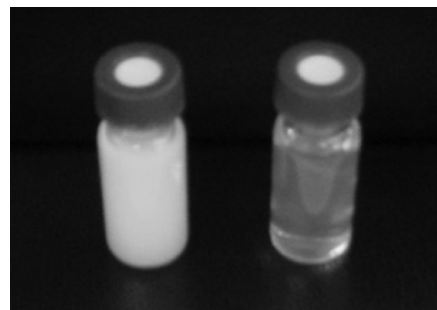


Figure 3. Chemically-initiated (left) and electron beam-initiated (right) PMMA latex.

mixer. The emulsion was then placed in the reaction cell and irradiated at 60 °C with a frequency of generally 10 Hz.

Conventional Polymerization. A typical chemically initiated emulsion polymerization was performed in a 300 mL double-walled glass reaction vessel with attached Teflon stirrer, reflux cooler, and gas inlet. First 150 mL of deionized water and 0.389 g of SDS were brought into the vessel, mixed at 400 rpm, purged with argon, and heated to 60 °C for 30 min. Then 15 g of monomer was added. The mixture was stirred for 45 min, allowing the monomer to emulsify. After formation of the emulsion, it was initiated with 0.3 g of SPS dissolved in 3 mL of water and polymerized over 3 h.

Results and Discussion

Chemically Initiated Emulsion Polymerization of MMA. Emulsion polymerization is today predominantly initiated by radicals produced through chemical initiation. To distinguish the difference between PEB initiation and chemical initiation at low surfactant concentrations, two PMMA latices at a surfactant concentration of 0.3 wt % (1.1×10^{-2} mol/L), slightly above the cmc of SDS, were polymerized. One PMMA latex was formed by chemical initiation with 8.4×10^{-3} mol/L SPS and the other by PEB irradiation of 267 kGy. The chemically initiated PMMA was opaque, whereas the PEB initiated latex was transparent (Figure 3).

The two latices showed two major differences in properties. The first one was the particle size. The chemically initiated PMMA had a particle size of around 60 nm, whereas the PEB initiated one had a particle size of 38.5 nm. This explains the difference in transparency of the two latices; the particle size of the PEB initiated PMMA was small enough to lead to transparency. The second difference was the molecular weight as found by SEC. The M_n of the chemically initiated PMMA was around 200 000, whereas the M_n of the PEB initiated PMMA was only about 12 000 (at a pulse repetition rate of 10 Hz).

To explain these differences, we will first have a closer look at the chemically initiated system. Higher surfactant concentrations in the system, above the cmc, lead to a larger number of micelles. With more micelles being present in the emulsion more loci of polymerization can be formed. The rate of polymerization increases with more loci of polymerization present in the system. When the same amount of monomer is distributed over a larger number of loci of polymerization, this results in smaller particle sizes. The particle size decreased at higher surfactant concentration, and consequently the particle number increased as can be seen in Table 1. Because the investigated surfactant concentrations were not high enough to form sufficiently small latex particles, none of the latices obtained were transparent.

PEB-Initiated Emulsion Polymerization of MMA. PEBP of MMA was performed in the 5 mL reaction cell

Table 1. Particle Size and Particle Numbers N_C for Chemically-Initiated Emulsion Polymerizations of MMA at Varying Surfactant Concentrations

surfactant concn (wt %)	particle size (nm)	N_C (L^{-1})
0.15	74	4.1×10^{17}
0.3	63	6.7×10^{17}
0.6	57	9.0×10^{17}
1.2	53	1.1×10^{18}

Table 2. Particle Size, Particle Numbers N_C , and Molecular Weights M_n for PEBP of MMA (10 Hz) at Varying Surfactant Concentrations Depending on the Conversion

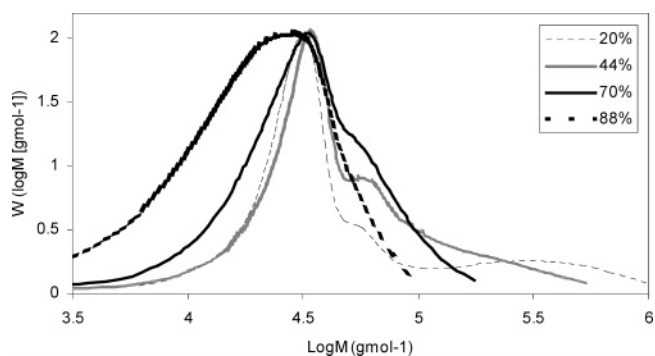
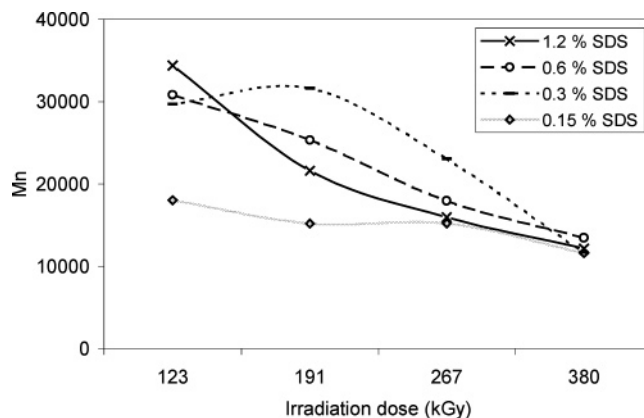
radiation dose (kGy)	conv (%)	particle size (nm)	N_C (L^{-1})	M_n
0.15 wt % SDS				
123	11	48	1.2×10^{17}	18 015
191	19	63	1.3×10^{17}	15 178
267	57	59	4.6×10^{17}	15 216
380	82	64	5.3×10^{17}	11 599
0.3 wt % SDS				
123	20	28	1.5×10^{18}	29 676
191	44	31	2.5×10^{18}	31 602
267	70	35	3.1×10^{18}	23 026
380	88	39	2.5×10^{18}	11 654
0.6 wt % SDS				
123	28	42	6.4×10^{17}	30 816
191	64	29	4.4×10^{18}	25 326
267	84	35	3.3×10^{18}	17 932
380	95	43	2.0×10^{18}	13 448
1.2 wt % SDS				
123	49	25	5.3×10^{18}	34 368
191	83	33	3.9×10^{18}	21 605
267	93	28	7.1×10^{18}	15 944
380	96	27	8.2×10^{18}	12 172

at surfactant concentrations varying between 0.15 and 1.2 wt % at 60 °C and a frequency of 10 Hz. At radiation doses between 123 and 380 kGy samples were taken. Table 2 gives the obtained data for the particle sizes, particle numbers, and molecular weights for the PEBP of MMA. The values for the particle size mildly fluctuate, reminding us that there is a continuous production of new particles but also some limited aggregation for these very small latex particles.

For the PEBP of MMA with SDS concentration between 0.3 and 1.2 wt % transparent latices were obtained; only the PEBP of MMA below the cmc, with 0.15 wt % SDS, gave opaque latex. The particles were smaller than in the chemically initiated system and the particle numbers larger (a factor of 5–10). On top of that effect, the PEBP logically showed larger particle sizes with increasing conversions.

SEC measurements verify the assumption of polymer decomposition during electron beam irradiation. Figure 4 shows the molar weight distribution (MWD) data of PEBP PMMA at different conversions/degrees of irradiation.

Figure 4 depicts a trimodal molar weight distribution of the PEB initiated PMMA at 20% conversion. The main peak ($M_{\text{peak}} = 30\,000$) has a shoulder of higher molecular weight material. The third peak of much higher molecular weight polymer (chains that escaped from termination several pulses) is small in size. As reaction and irradiation time increases, the intensities of the higher molecular weight peaks decrease. At 88% conversion and 380 kGy both higher molecular weight peaks have disappeared. The amount of low molecular weight material has increased. These results show that

**Figure 4.** MWD spectra of an electron beam-initiated PMMA polymerized with an SDS concentration of 0.3 wt % at 60 °C and a frequency of 10 Hz measured at various degrees of conversions (irradiation doses between 123 and 380 kGy).**Figure 5.** M_n of PEB-initiated PMMA latex (at frequency of 10 Hz) polymerized with various SDS concentrations (between 0.15 and 1.2%) at 60 °C measured at different radiation doses and thus conversions.

PEB irradiation breaks up high molecular weight PMMA molecules. The chain decomposition is also reflected in the final molecular weights M_n of the obtained latices (Table 2).

Figure 5 shows how the molecular weight of latices, polymerized with various surfactant concentrations, decreased with increasing radiation doses. This effect can be attributed to the decomposition of longer PMMA chains over irradiation time, in combination with the decrease in monomer concentration. The final conversion of the latices was generally 90–95%.

The analysis of the trimodal peak for 20% conversion polymerized at 10 Hz in Figure 4 shows the typical size distribution of a pulsed initiation polymerization (eq 1). Figure 6 displays the SEC molecular weight distribution and the first derivative of the curve.

The inflection points $L_{0,i}$ of the log M curve are determined by the peak maxima of first derivative of the curve. $L_{0,i}$ represents the average chain length a radical can grow within i and $i + 1$ pulses during the time interval t .⁹ Table 3 lists the values for the first and second inflection point. The values in Table 3 represent the M values for chains initiated with one pulse and terminated by the next pulse or by the next plus one pulse.

Table 3 shows that M for the second inflection point $L_{0,2}$ has twice the value of M at the first inflection point, $L_{0,1}$. This confirms that the experimental results obey the rules of pulsed initiation polymerization as it obeys the IUPAC reliability criteria for pulsed initiation polymerizations.¹⁰

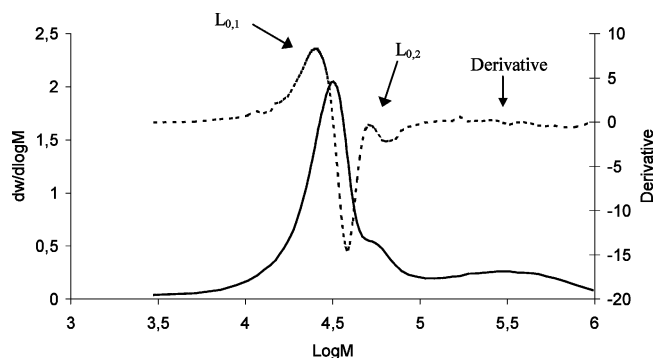


Figure 6. MWD spectra of PEBP PMMA latex at 20% conversion (irradiation dose of 123 kGy), polymerized with 0.3% SDS at a frequency of 10 Hz and 60 °C and the first derivative of the MWD.

Table 3. Maxima of the First Derivative of $\log M$, $L_{0,i}$, and the Corresponding Molecular Mass (M) for a PEB (10 Hz)-Initiated PMMA Latex with 20% Conversion Irradiated with 123 kGy

	$\log M$	M
$L_{0,1}$	4.4045	25 380
$L_{0,2}$	4.7058	50 792

Equation 1 for the kinetic chain length L allows calculation of the monomer concentration at the locus of polymerization.

$$L = k_p[M]t \quad (1)$$

The calculated value of 2.6 mol/L was found earlier in PEBP of MMA at conversions around 20% (2.7 mol/L at 22% conversion at similar conditions and particle sizes), indicating that the loci of polymerization were predominantly the latex particles or the monomer droplets.¹¹ Similar analysis obtained comparable results for latices polymerized at different surfactant concentrations after irradiation with 123 kGy. At higher radiation doses the chain decomposition strongly affected the pattern of the MWD (see Figure 6). The analysis of those latices therefore cannot be used to obtain estimates for the monomer concentration based on eq 1.

The obtained value for the swellability of PMMA in MMA is lower than the recorded 6.6 mol/L for particle sizes of 70 nm and higher.¹² Gilbert has shown in calculations using the Vanzo equation for PSty that the monomer solubility in polymer latex particles decreases for smaller particle sizes.^{1,13} The reason for this is the contribution of the surface energy to the chemical potential of the monomer in the particle phase. The calculations resulted in a solubility of Sty in PSty of 5.5 mol/L for particles of 100 nm and less than 4 mol/L for 30 nm particles. The same effect of decreasing polymer swellability with decreasing latex diameter is expected to take place in the case of MMA/PMMA.

PEB-Initiated Emulsion Polymerization of EMA.

Ethyl methacrylate (EMA) has a similar chemical structure as MMA, but because of the additional methylene group it is less water-soluble. EMA was polymerized at low surfactant concentrations with PEB initiation to investigate the effect of water solubility of the polymerized monomer on the PEBP.

The PEBP of EMA with surfactant concentrations of 0.15 and 0.3 wt % SDS resulted in inhomogeneous latices. Larger amounts of coagulate precipitated on the wall of the reaction cell. Phase separation of the primary

Table 4. Conversion, Particle Size, and Molecular Weights M_n for PEBP (10 Hz) of EMA with Two Surfactant Concentrations and Different Radiation Doses

radiation dose (kGy)	conv (%)	particle size (nm)	M_n
0.15 wt % SDS			
123	23	55	18 460
191	20	48	17 106
267	44	57	20 294
380	59	80	17 501
0.3 wt % SDS			
123	41	132	28 153
191	49	99	21 189
267	67	41	19 827
380	76	86	17 326

Table 5. Conversion, Particle Size, and Molecular Weights M_n for PEBP (10 Hz) of BMA with Two Surfactant Concentrations and Different Radiation Doses

radiation dose (kGy)	conv (%)	particle size (nm)	M_n
0.15 wt % SDS			
123	14	54	16 942
191	30	72	19 335
267	34	53	18 867
380	46	50	20 642
0.3 wt % SDS			
123	63	149	42 409
191	69	116	40 671
267	81	109	28 227
380	76	103	24 561

opaque latices was observed and resulted in a small layer of opaque material on the surface of the barely transparent latex. The emulsion was obviously not stable. The conversion rates of EMA were surprisingly similar to those of MMA (Table 4). Because of the inhomogeneity of the latices, their measured particle sizes show large variations. Similar to the observations for the PEBP of MMA, the molecular weights of the PEMA decreased at higher radiation doses, indicating polymer chain decomposition.

Because of the poor water solubility of EMA, the initiation in micelles, particles, and monomer droplets with monomer radicals plays a more important role than nucleation through oligomer formation (in the case of the better water-soluble MMA⁴). This effect can lead to the formation of less and thus larger latex particles and thus opaque latex where also the amount of surfactant is insufficient to stabilize the produced latex.

PEB-Initiated Emulsion Polymerization of BMA.

The PEBP of butyl methacrylate (BMA) confirms the effect of the water solubility of the polymerized monomer in PEBP as seen before with MMA and EMA. Because of its butyl group, BMA is less water-soluble than MMA and EMA. The polymerization of BMA at surfactant concentrations of 0.15 and 0.3 wt % SDS resulted, similar to the PEBP of EMA, in inhomogeneous latices. Larger amounts of coagulate precipitated on the wall of the reaction cell.

The opaque latices obtained primary turned after storage into a two-phase system with small amounts of opaque material on the surface of barely transparent latex. The conversion rates of BMA were similar to those of MMA and EMA. Because of the inhomogeneity of the latices, the measured particles varied broadly in size (Table 5). The molecular weights showed similar tendencies as PEBP of MMA and EMA. Larger molecular

Table 6. Particle Sizes of a PEB (10 Hz)-Initiated PVAc Latex Containing 0.3 wt % SDS Irradiated with Various Electron Beam Doses

radiation dose (kGy)	conversion (%)	particle size (nm)
123	88	34
191	94	33
267	91	28
380	95	30

weights were broken down at high radiation doses. The polymerization of BMA at 0.3 mol/L SDS resulted in unusually high molecular weights compared to the PEBP of MMA and EMA.

The PEB initiation of BMA showed the same effects as seen with EMA. Because of the poor water solubility, a relatively small number of formed latex particles were observed.⁴

PEB-Initiated Emulsion Polymerization of VAc.

To allow a comparison with the obtained data for PEBP of MMA, EMA, and BMA, vinyl acetate (VAc) was polymerized under the same conditions. VAc is moderately water-soluble (5.0×10^{-1} mol L⁻¹, see Table 9). The latices obtained from the PEBP of VAc are more or less transparent with transmissions of e.g. 66.5% at 450 nm, 70.6% at 550 nm, and 83.9% at 650 nm. Overall, these lattices appeared to be slightly less transparent as compared to the PMMA latices. The data in Table 6 show the high polymerization rates of VAc. The average particle sizes were in the range of 30 nm.

PVAc is known to easily undergo chain transfer reactions.^{14–16} Chain transfer to monomer and chain transfer to polymer led to branching and cross-linking of the polymer. Higher temperatures enhance these reactions. Because of these reactions, also cross-linking of the PEB irradiated PVAc occurred, which made it impossible to analyze the latices with SEC.

PEB-Initiated Emulsion Polymerization of Sty.

Another well-investigated monomer, Sty, was polymerized under the same conditions with PEB initiation as MMA, EMA, BMA, and VAc. The water solubility of Sty is low as can be seen in Table 9. Sty was very interesting in our investigations because it is known not to decompose under irradiation. Irradiation tests with chemically initiated PSty standards indeed showed no polymer degeneration and confirmed the observations of Sato et al.¹⁷

The PEBP of Sty yielded inhomogeneous latices that appeared primarily opaque and turned into a two-phase system: bluish slightly transparent latex with a small amount of foamy liquid on top. Coagulation was again observed on the walls of the reaction cell, and no conversion higher than 20% could be reached. Chapiro et al. explained low conversions with the observation that even traces of oxygen retarded the PEBP of Sty.¹⁸ Because it was not possible to exclude oxygen in the batch setup, this also might have been the cause of low conversions in our case.

Comparison of Primary Radical Formation, Water Solubility, and k_p of Monomers in PEB-Initiated Emulsion Polymerization. To explain the obtained results, a detailed comparison of G values, water solubility, and k_p of the polymerized monomers needs to be carried out.

G values are defined as the number of species created with 100 eV of absorbed dose. The G values of water, MMA, and Sty are given in Table 7.

Table 7. G Values of Species Present in a Typical Emulsion Polymerization¹⁹

reactant species	product species	G value
H ₂ O	H radical	0.57
H ₂ O	OH radical	2.70
H ₂ O	e _{aq} ⁻	2.75
Sty	Sty radical	0.69
MMA	MMA radical	5.50

^a Hydrated electron.

Table 8. Primary Radicals Formed with One PEB at Zero Conversion with a Dose of 76 Gy

radical	$C_0^R(\text{Sty})$ (mol L ⁻¹)	$C_0^R(\text{MMA})$ (mol L ⁻¹)
monomer _{aq} [*]	2.3×10^{-9}	6.0×10^{-7}
monomer _{droplet} [*]	5.6×10^{-7}	3.9×10^{-6}
H [*]	4.2×10^{-6}	4.2×10^{-6}
OH [*]	1.9×10^{-5}	1.9×10^{-5}
e _{aq} ⁻	2.0×10^{-5}	2.0×10^{-5}
total	4.4×10^{-5}	4.7×10^{-5}
% in the aq phase	99	92
% with OH	43	40

Table 9. Water Solubility, Propagation Rate Coefficient, and Their Product of Selected Monomers²¹

monomer	[M] _{aq} (20 °C) (mol L ⁻¹)	k_p (50 °C) (L mol ⁻¹ s ⁻¹)	$k_p[M]_{aq}$ (s ⁻¹)
MMA	1.5×10^{-1}	649	97
EMA	6.5×10^{-2}	676	44
BMA	2.5×10^{-3}	857	2.1
Sty	4.3×10^{-3}	237	1.0
VAc	5.0×10^{-1}	7540	3770
BA	2.5×10^{-3}	40400	101

To calculate the radical concentrations in the reaction, one has to take the following into account: The G value is the number of species created per 100 eV or rather 1.6×10^{-17} J. The applied radiation source had an energy E of 0.39 J per pulse. Therefore, $G \times 2.44 \times 10^{16}$ species were created per pulse. Divided by Avogadro's number N_A of 6.022×10^{23} mol⁻¹ and the reactor volume (0.005 L) and multiplied with the relative amount of one reactant to the reaction mixture x_i , one ends up with eq 2 for the initial radical concentration C_0^R of a species i :

$$C_{0,i}^R = 8.1 \times 10^{-6} \text{ mol L}^{-1} G_i x_i \quad (2)$$

The relative amount of the monomers in water and in the monomer droplets and micelles in Table 8 are calculated with the water solubility of the investigated monomers given in Table 9.

The data in Table 8 only cover the radical formation for an initial electron pulse that hits the emulsion. Further calculation of the radical concentrations during the proceeding polymerization turns out to be rather complicated for all propagating species. But nevertheless calculations provide an idea about the high radical flux that is created within PEBP and underlines the efficiency of one electron pulse. Note that no G values for SDS were recorded. Because the concentration of the surfactant is low in the emulsion, relatively only a low number of radicals formed from SDS are expected. MALDI-TOF MS showed, except for the PEBP of Sty, no evidence of appearance of end groups that could be attributed to possible SDS fragmentation products.⁴

The data in Table 8 depict that a high radical concentration is formed per pulse. In chemically initiated systems the SPS concentration was 9.8×10^{-3} mol L⁻¹, a value in the range commonly used. The k_d of SPS

is $3.1 \times 10^{-5} \text{ s}^{-1}$ at $60 \text{ }^\circ\text{C}$, which leads to an initial radical formation of around $3.0 \times 10^{-7} \text{ mol s}^{-1} \text{ L}^{-1}$.²⁰ In the PEBP of MMA at 10 Hz a radical formation of $4.7 \times 10^{-4} \text{ mol s}^{-1} \text{ L}^{-1}$ was calculated (Table 8), i.e., 1000 times more than in the chemically initiated polymerization with SPS, indicating a high radical flux in the PEBP system.

Table 8 also shows that the majority of radicals are formed in the water phase, resulting in a low rate of oligomer production, explaining the low conversions for the PEBP of Sty. The significant proportion of OH radicals confirms findings seen in MALDI-TOF MS that a high amount of hydroxyl functional polymer is formed in the PEBP of e.g. MMA.⁴ This high amount of hydroxyl functions in the polymeric chain is expected to stabilize the transparent latices with small particle sizes. Because the amount will be lower for less water-soluble monomers, the stabilization of rather small particles of those monomers will decrease.

As seen in the end-group analysis with MALDI-TOF MS, the initiation in PEBP will predominantly start in the aqueous phase due to the high radical formation there.⁴ The propagation of the oligomers occurs in the water phase until the oligomers reach the chain length, at which they become surface active and can enter a particle or after further propagation form a new particle. Two factors have a great impact on the polymerization kinetics: the water solubility and the propagation rate coefficient of the monomer; the product determines the reaction rate. The values for water solubility and propagation rate coefficient of the examined monomers are given in Table 9.²¹

Because of the high radical flux in the PEBP, a high number of radicals will be formed in the aqueous phase. If a monomer, like VAc or MMA, has a high propagation rate and a relatively high water solubility, the oligomer radicals will propagate very fast in the aqueous phase, and thus a high number of particles will be formed. Because of the high degree of hydroxyl functions in the polymeric chains, the polymer will be able to form stable small particles, yielding transparent latex even at low surfactant concentrations.

Low water solubility of the monomer will affect PEBP; the aqueous phase propagation will decrease, fewer particles will be formed over time, and thus the rate of polymerization will decrease. When the polymerization is performed at very low surfactant concentrations like in the experiments shown, this effect will lead to a decrease in the system stability over time, resulting in coagulum formation and/or phase separation as seen for EMA, BMA, or Sty.

Experiments with butyl acrylate (BA) showed that PEBP of BA could form transparent latices.¹¹ Although the water solubility of BA is poor ($2.5 \times 10^{-3} \text{ mol L}^{-1}$), the k_p ($40\,400 \text{ L mol}^{-1} \text{ s}^{-1}$) is very high, which provides sufficient aqueous phase propagation of the oligomers and the formation of a high amount of hydroxyl functionalities stabilizing small particles.

Thus, the product of k_p and the water solubility of the monomers (Table 9) can give an appropriate estimation of the chance of a monomer to form a transparent latex in PEBP at low surfactant concentrations. When the product of k_p and the water solubility is low, the chance of preparing a transparent latex is low.

A high concentration of OH radicals formed in the PEBP due to the high radical flux in the system also affects the formation of transparent latices. The OH

radicals initiate polymerization and form oligomer chains with hydroxyl functions. In microemulsion polymerizations short-chained hydroxyl-functionalized molecules, like e.g. 1-pentanol, are added to the recipe as a cosurfactant to obtain small particle sizes.² Only monomers with a relatively high water solubility (MMA, VAc) or a high propagation rate coefficient (VAc, BA) were able to form stable transparent latices. This explains the production of transparent latices of MMA, VAc, and BA. The method is performed at relatively low solid contents and small scale. Scale-up of the method is possible but limited. The attainable solid contents would be around 30% solids after optimization of the reactor geometry, making a concentration step unnecessary.

Conclusions

The pulsed electron beam (PEB)-initiated emulsion polymerization of methyl methacrylate (MMA) at low surfactant concentrations yields latices with properties different from those of the chemically initiated MMA. Whereas the PEB-initiated latices were transparent in principle, the chemically initiated PMMA latices appeared to be opaque. Three main differences between PEB-initiated and chemically-initiated PMMA, which are crucial to latex transparency, can be identified. In the first place is the particle size. The 30 nm sized PEB initiated latex particles were transparent whereas the 60 nm sized latex, initiated chemically, came out opaque. The high radical flux in the PEB-initiated system created a higher particle number, resulting in smaller particles. Second, PEB-initiated PMMA had low molecular weights (peak maximum at around 30 000 Da) compared to chemically-initiated PMMA with molecular weights of a few hundred thousand. The third difference was the high number of hydroxyl-functionalized PMMA chains in the PEB initiated latices due to polymerization initiation with OH radicals. The presence of many hydroxyl-functionalized PMMA chains (especially at low molecular weight) seemed to colloidal stabilize the small latex particles and to prevent coagulation. Note that coagulation usually occurs at low surfactant concentrations. Hydroxyl-functional oligomers also might have favored the production of small particles, positively acting as cosurfactant similar as in microemulsion polymerizations. The comparison of PEB initiation of a series of monomers, viz. MMA, ethyl methacrylate (EMA), butyl methacrylate (BMA), styrene (Sty), and vinyl acetate (VAc), revealed that water-phase propagation rate and therefore the water solubility and the propagation rate coefficient of the monomers affect the number of oligomers produced in the aqueous phase and therefore the size of the particles of the obtained latex. Poorly water-soluble monomers like EMA, BMA, and Sty with low propagation rate coefficients did not form transparent latices in PEB-initiated polymerizations.

References and Notes

- (1) Gilbert, R. G. *Emulsion Polymerisation, a Mechanistic Approach*; Academic Press: San Diego, 1995.
- (2) Guo, J. S.; El-asser, M. S.; Vanderhoff, J. W. *J. Polym. Sci., Part A* **1989**, *27*, 691.
- (3) Stahel, E. P.; Stannett, V. T. In *Large Radiation Sources for Industrial Processes*; International Atomic Energy Agency: Vienna, 1969.
- (4) Pusch, J.; van Herk, A. M. Pulsed Electron Beam Initiation in Emulsion Polymerisation, submitted for publication.
- (5) Beuermann, S.; Paquet, D. A., Jr.; McMinn, J. H.; Hutchinson, R. A.; *Macromolecules* **1996**, *29*, 4206.

- (6) Botman, J. I. M.; Derksen, A. T. A. M.; van Herk, A. M.; Jung, M.; Kuchta, F.-D.; Manders, L. G.; Timmermans, C. J.; de Voigt, M. J. *Nucl. Instrum. Methods Phys. Res., Sect. B* **1998**, *139*, 490.
- (7) Van Duijneveldt, W.; Botman, J. I. M.; Timmermans, C. J.; De Leeuw, R. W. *Nucl. Instrum. Methods Phys. Res., Sect. B* **1993**, *79*, 871.
- (8) Derksen, A. T. A. M.; Timmermans, C. J.; Wintraeken, Y. J. E.; Botman, J. I. M.; Fiedler, H.; Hagedoorn, H. L. *Proc. 5th Eur. Particle Accelerator Conf. Barcelona, Spain* **1996**, 2699.
- (9) Olaj, O. F.; Bitai, I.; Hinkelmann, F. *Macromol. Chem.* **1987**, *188*, 1698.
- (10) Buback, M.; Gilbert, R. G.; Hutchinson, R. A.; Klumperman, B.; Kuchta, F.-D.; Manders, B. G.; O'Driscoll, K. F.; Russell, G. T.; Schweer, J.; *Macromol. Chem. Phys.* **1995**, *196*, 10, 3267.
- (11) Internal Report TUE/Rhom & Haas, 1999.
- (12) Ballard, M. J.; Napper, D. H.; Gilbert, R. G. *J. Polym. Sci., Polym. Chem. Ed.* **1984**, *22*, 3225.
- (13) Vanzo, E.; Marchessault, R. H.; Stannet, V. J. *J. Colloid Sci.* **1965**, *20*, 62.
- (14) Nozakura, S.-I.; Morishima, Y.; Murahashi, S. J. *J. Polym. Sci., Part A* **1972**, *10*, 2853.
- (15) Melville, H. M.; Sewell, P. R. *Makromol. Chem.* **1959**, *32*, 139.
- (16) Dunn, A. S.; Naravane, S. R. *Br. Polym. J.* **1980**, 75.
- (17) Sato, K.; Rudin, A.; Huang, R. Y. M. *J. Polym. Sci., Polym. Chem. Ed.* **1976**, *14*, 37.
- (18) Chapiro, A. *Radiation Chemistry of Polymeric Systems*; John Wiley & Sons: London, 1962; p 173.
- (19) <http://physics.nist.gov/PhysRefData/Star/Text/ESTAR.html>.
- (20) Kolthoff, I. M.; Miller, I. K. *J. Am. Chem. Soc.* **1951**, *73*, 3055.
- (21) *Course on Emulsion Polymerisation*; Script, SEP: Eindhoven, 2001.

MA0502001